Active Vibration Control Synthesis for the Control of Flexible Structures Mast Flight System

Bong Wie
University of Texas at Austin, Austin, Texas

Pole-zero modeling and active vibration control synthesis for the Control of Flexible Structures Mast Flight System (COFS-I) are discussed. An analytical transfer function from the tip-mounted actuator force to the beam deflection at various sensor locations is derived for control synthesis. A new concept of generalized structural filtering for flexible-mode stabilization is applied to the COFS-I. The simplicity and practicality of the classical transfer-function approach to active structural vibration control are demonstrated for the COFS-I. In particular, nonminimum-phase structural filtering is proposed for the noncolocated control experiment of the COFS-I. The effects of proof-mass actuator dynamics and control-loop time delay on the phase/gain stabilization of the flexible modes are also discussed.

Introduction

THE objective of this paper is to present the major findings and results obtained for the proposed control experiment of the COFS (Control of Flexible Structures) project.[1] Mathematical modeling, active vibration control synthesis, and digital simulation results for the proposed control experiment are discussed. These preliminary investigation results will make significant contributions toward establishing flight-ready control technologies for the COFS experiments. In particular, this paper demonstrates the practical usefulness of the classical transfer-function approach to active structural vibration control synthesis.

The COFS-I flight article (the Mast Flight System) described in Ref. 1 consists primarily of a beam structure with 275-kg distributed mass (including the 93-kg distributed mass of control hardware) and a 180-kg tip mass. The COFS-I deployed configuration and the distributed actuator/sensor locations are illustrated in Fig. 1; a simplified geometry and a summary of the material properties are given in Fig. 2. Since this beam structure with significant tip mass is cantilevered to the Orbiter, the overall transient responses are dominated by the first flexible mode in each axis. The 2-Hz second bending mode is widely separated from the 0.2-Hz first bending mode and has an order of magnitude less modal contribution than the first mode. Consequently, the COFS-I flight article does not have the closely spaced modal characteristics expected for future large structures in space. It has, however, some closely spaced natural frequencies that are the frequencies of the bending modes in the orthogonal axes.

On the other hand, the COFS-I represents a typical control/structure interaction problem where controlling the primary modes always requires consideration of the control interactions with the secondary modes. When using a colocated actuator/sensor pair, a stable interaction exists; however, special consideration must be given to the *unstable* interaction when the actuator and sensor are not colocated. In this paper, the first bending mode is considered as a primary mode to be actively damped. The second and higher bending modes are considered as the secondary modes that are not to be destabilized by the primary-mode controller. Two candidate control objectives for the COFS-I flight experiment are : 1) a rapid transient control of the tip deflection to an impulse-type disturbance, and 2) a steady-state vibration suppression to broadband or narrow-band disturbances. Only the rapid transient vibration control is considered in this paper with a special emphasis on the active damping control using a noncolocated actuator/sensor pair.

Preliminary control synthesis results are presented for two different generic cases: 1) a colocated control using the tip-mounted primary actuator/sensor pair, and 2) a noncolocated control using the tip-mounted actuator and noncolocated sensor. The proof-mass actuator dynamics with 1-Hz high-pass break frequency and an effective control loop delay of 10 ms are assumed.[1] The COFS-I is modeled as a uniform cantilevered beam with a tip mass. Using the analytical modeling approach in Refs. 2–6, a transcendental transfer function with exact poles and zeros is derived for arbitrary deployed lengths for control synthesis. It is, however, emphasized that this analytical model is essentially a qualitative representation of the actual truss structure. For the noncolocated actuator/sensor control of the COFS-I, the new generalized structural filtering concept[7] is employed to phase-stabilize the second bending mode. This new concept is a generalization of the classical notch and phase lead/lag filters.[8–11] Although this concept can also be extended to the multi-input/multi-output

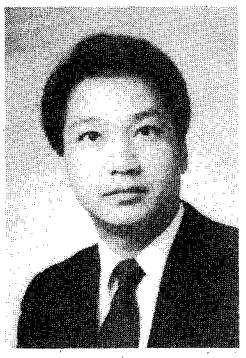

Bong Wie was born in Seoul, Korea, on February 25, 1952. He received a B.S. degree in Aeronautical Engineering from Seoul National University in 1975, and M.S. and Ph.D. degrees in Aeronautics and Astronautics from Stanford University, in 1978 and 1981, respectively. From 1981 to 1985, he was employed as a control/dynamics analyst at the Ford Aerospace & Communications Corporation. In 1985, he joined the faculty of the University of Texas at Austin, where he is currently an Assistant Professor in the Department of Aerospace Engineering and Engineering Mechanics. His research interests include spacecraft control and dynamics, control systems synthesis, and modeling and control of large space structures. He is an Associate Editor for the *Journal of Guidance, Control, and Dynamics*. He is a Member of AIAA and is a consultant to the Ford Aerospace & Communications Corporation.

Presented as Paper 87-2322 at the AIAA Guidance, Navigation, and Control Conference, Monterey, CA, Aug. 17–19, 1987; received April 3, 1987; revision received July 31, 1987. Copyright © American Institute of Aeronautics and Astronautics, Inc., 1987. All rights reserved.

control design when the classical "successive-loop-closure" approach[12,13] is employed, only the single-input/single-output control problem is discussed.

COFS-I Flight System Description

In this section the COFS-I system is briefly reviewed for the purposes of a preliminary control design. As illustrated in Fig. 2 the basic element of the COFS-I is a 60-m-long, triangular-cross-sectioned, joint-dominated truss structure; an approximately 180-kg tip mass includes primary actuators/sensors and a Parameter Modification Subsystem (PMS). A tip-mounted PMS can vary the beam parameters to adjust the frequency spacing and coupling of the second bending mode and the first torsion mode.[1] Using the PMS the frequency can be continuously adjusted to provide less than 3% separation. However, the coupling of the second bending mode and the first torsion mode is not considered in this paper, because the second bending mode has an order of magnitude less modal contribution than the first bending mode.

Both primary and secondary actuators are included with certain sensors and a computer in an Excitation and Damping Subsystem (EDS). The sensors include both tip-mounted rate gyros and accelerometers distributed at various locations. The EDS computer is a MIL SPEC 1750A processor capable of executing 600,000 instructions per second; the floating-point multiply time is 3.5 μs; the total memory is 128K of 16-bit words; the sensors and the computer have 150-Hz sampling rate (6.6-ms sampling period). For a preliminary analysis, an effective delay of 10 ms is assumed.

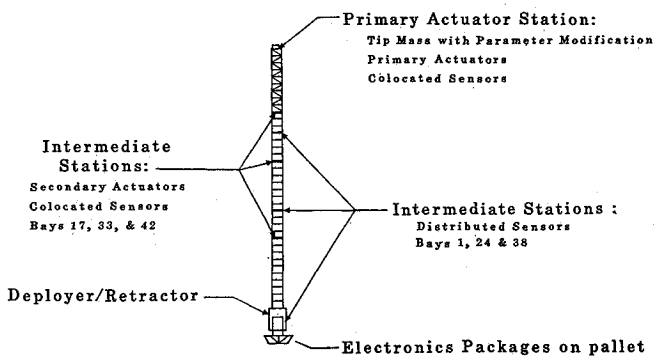

Fig. 1 The COFS-I flight system deployed configuration.

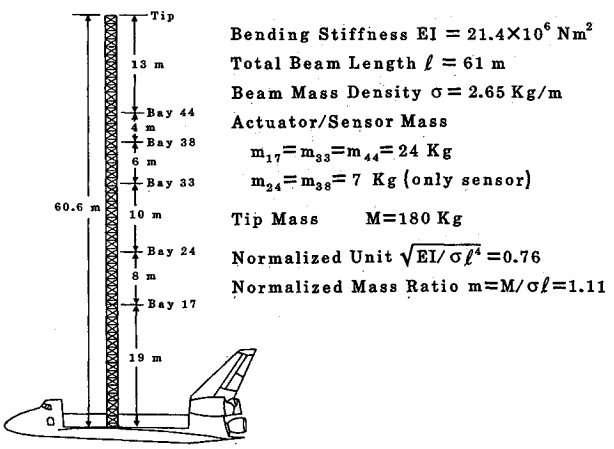

Fig. 2 The COFS-I simplified geometry and material properties.

Pole-Zero Modeling

The COFS-I has only one dominant mode in each axis since the beam structure with significant tip mass is cantilevered to the Orbiter. As a result, controlling the beam vibration using only the tip-mounted primary actuator is considered in this paper. An analytical transfer function from the control force input to the deflections at various points on the beam structure can be determined using the analytical approach used in Refs. 2–6. Transfer functions from an actuator located other than at the tip can also be determined using the transfer-matrix method described in Ref. 2. The additional lumped mass at bays 17, 24, 33, 38, and 44 (see Fig. 1) is neglected for the preliminary analytical modeling herein. This analytical modeling approach provides a qualitative representation of the actual beam structure. It also provides physical insights to the modeling and control problems of the COFS-I control experiment.

For a uniform cantilevered beam with a tip mass M, the equation of motion is

$$EIy''''(x,t) + \sigma\ddot{y}(x,t) = 0 \tag{1}$$

where

$$y'''' \triangleq \frac{\partial^4 y}{\partial x^4}$$

and

$$\ddot{y} \triangleq \frac{\partial^2 y}{\partial t^2}$$

The transverse deflection is $y(x,t)$ at the location x and time t; EI, σ, and ℓ are the bending stiffness, mass density, and total length of the beam, respectively.

The boundary conditions are

$$y(0,t) = y'(0,t) = 0 \tag{2a}$$

$$y''(l,t) = 0 \tag{2b}$$

$$M\ddot{y}(l,t) - EIy'''(l,t) = u(t) \tag{2c}$$

where M is the tip mass and $u(t)$ the proof-mass actuator control force.

Taking the Laplace transforms of Eqs. (1) and (2) we get

$$y''''(x,s) - \lambda^4 y(x,s) = 0 \tag{3}$$

where $\lambda^4 = -s^2$, s in units of $\sqrt{EI/\sigma l^4}$, and

$$y(0,s) = y'(0,s) = 0 \tag{4a}$$

$$y''(1,s) = 0 \tag{4b}$$

$$-m\lambda^4 y(1,s) - y'''(1,s) = u(s) \tag{4c}$$

where $m = M/\sigma l$, x and y in units of l, and u in units of EI/l^2.

The solution of Eq. (3) is given by

$$y(x,s) = A_1 \sin(\lambda x) + A_2 \cos(\lambda x) + A_3 \sinh(\lambda x) + A_4 \cosh(\lambda x) \tag{5}$$

By combining Eqs. (4) and (5) we get the transcendental transfer functions from the control force $u(s)$ to the beam deflection $y(x,s)$ and to the beam slope $y'(x,s)$ at location x

$$\frac{y(x,s)}{u(s)} = \frac{(c\lambda + ch\lambda)(s\lambda x - sh\lambda x) - (s\lambda + sh\lambda)(c\lambda x - ch\lambda x)}{2\lambda^3(1 + c\lambda ch\lambda) + 2m\lambda^4(c\lambda sh\lambda - s\lambda ch\lambda)} \tag{6a}$$

$$\frac{y'(x,s)}{u(s)} = \frac{\lambda(c\lambda + ch\lambda)(c\lambda x - ch\lambda x) + \lambda(s\lambda + sh\lambda)(s\lambda x + sh\lambda x)}{2\lambda^3(1 + c\lambda ch\lambda) + 2m\lambda^4(c\lambda sh\lambda - s\lambda ch\lambda)} \tag{6b}$$

where $s(\ ) = \sin(\ )$, $c(\ ) = \cos(\ )$, $sh(\ ) = \sinh(\ )$, and $ch(\ ) \triangleq \cosh(\ )$, for brevity.

In particular, the transfer functions from the tip-mounted primary actuator to the tip deflection and to the tip slope become

$$\frac{y(1,s)}{u(s)} = \frac{s\lambda ch\lambda - c\lambda sh\lambda}{\lambda^3(1 + c\lambda ch\lambda) + m\lambda^4(c\lambda sh\lambda - s\lambda ch\lambda)} \tag{7a}$$

$$\frac{y'(1,s)}{u(s)} = \frac{\lambda s\lambda sh\lambda}{\lambda^3(1 + c\lambda ch\lambda) + m\lambda^4(c\lambda sh\lambda - s\lambda ch\lambda)} \tag{7b}$$

By determining the roots of the numerator and denominator of these transfer functions for given tip-mass ratio of m, these transcendental transfer functions can be represented as infinite products of poles and zeros. For example, Eq. (7a) can be written as

$$\frac{y(1,s)}{u(s)} = \frac{\prod_{i=1}^{\infty}\left[\frac{s^2}{z_i^2} + 1\right]}{\prod_{i=1}^{\infty}\left[\frac{s^2}{p_i^2} + 1\right]} \tag{8}$$

where modal terms can be added directly to both numerator and denominator.

Since the control of tip deflection is the primary consideration in this paper, Eq. (7a) is further discussed here. It is observed that the transfer-function zeros are independent of the tip-mass ratio m, while the poles (natural frequencies) are dependent on the mass ratio. The zeros of Eq. (7a) are the natural frequencies of a clamped-hinged beam; the poles and zeros of Eq. (7a) for different values of the mass ratio are shown in Fig. 3. The poles and zeros are alternating along the imaginary axis, which is the property of the colocated actuator and sensor. For $m = 0$ (no tip mass) each mode, except for the first mode, has a well-separated pole-zero pair. As m increases, the poles and zeros associated with the second and higher bending modes become closely spaced and the first mode becomes a single dominant mode of the cantilevered beam. Since the frequencies in Fig. 3 are in units of $\sqrt{EI/\sigma l^4}$, they should be multiplied by 0.76 to become frequencies in units of rad/s for a fully deployed configuration. For $m = 1$, the lowest four natural frquencies become 0.18, 1.96, 6.14, 12.7 Hz (or 1.14, 12.31, 38.6, 79.8 rad/s), which are in close agreement with the NASTRAN data given in Ref. 1. An 8th-order transfer-function model with a $\pm 25\%$ pole-zero uncertainty and with a 0.002 passive damping ratio is assumed here as a preliminary control design model.

Figure 4 shows the poles and zeros of transfer functions from the tip-mounted actuator force to the beam deflection at various secondary sensor locations. Since the actuator and the sensor are not colocated in this case, the poles and zeros are not alternating along the imaginary axis. This transfer-function zero locations are sensitive to the actual mode shapes; the transfer function to the deflection at the bay 17 ($x = 0.313$) has no zeros associated with the lowest four modes. A case of controlling the beam vibration using the tip-mounted actuator and the sensor at bay 33 is selected because the second mode has a maximum deflection at bay 33.

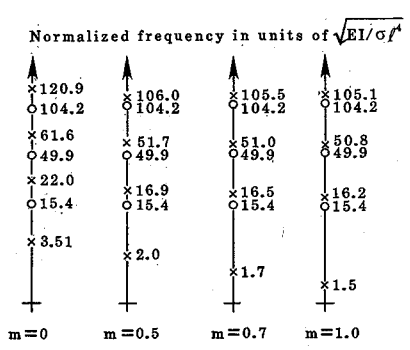

Fig. 3 Poles and zeros of the transfer function from the tip actuator to the tip deflection for different values of the tip-mass ratio.

Proof-Mass Actuator Dynamics

The proof-mass force actuator implemented as a linear dc motor is the primary actuating device for the COFS-I control experiment. Detailed static characteristics of the actuator can be found in Ref. 1. The low-frequency dynamic characteristics of this proof-mass actuator are discussed here for control applications.

The proof-mass actuator can be considered as the translational equivalent to the reaction wheel that is one of the primary actuating devices for attitude control of spacecraft. The proof-mass actuator applies force, while the reaction wheel applies torque. Similar to those of the reaction wheel[9] or the control-moment gyros,[14] the proof-mass actuator dynamics can be modeled as a high-pass filter. An integral of the velocity (i.e., a structural displacement) should be used for feedback to the velocity-controlled proof-mass actuator for active vibration control. In order to eliminate any biases in the control signal this integration must be implemented as a compensation of the type $s/(s + a)(s + b)$ where a and b are small compared to the frequency of the lowest mode to be controlled.[15]

The Laplace-transformed equations of motion of a velocity-controlled linear proof-mass actuator can be written as[15]

proof-mass dynamics

$$ms^2(q + y) + kq = -u \tag{9a}$$

structural dynamics

$$y = G(s)u \tag{9b}$$

actuator control force

$$u = -K(v - sq) \tag{9c}$$

where m is the mass of the proof-mass, k the spring stiffness of the suspension system, and q the relative displacement of the proof-mass with respect to the structure that has inertial displacement of y. The $G(s)$ is a trnasfer function of the structure [e.g., Eq. (6) or (7)], K the velocity-controlled actuator servo gain, and v the proof-mass velocity command.

An actuator transfer function from the commanded velocity v to the output velocity sq can then be found as

$$\frac{sq}{v} = \left[1 + \frac{ms^2 + k}{Ks(1 + ms^2G(s))}\right]^{-1} \tag{10}$$

For a high-servo-gain K, the output velocity sq follows the commanded velocity-input v. If the structural displacement y is relatively small compared to the displacement of the proof-mass, then we have

$$u = -ms^2q \tag{11}$$

If the structure transfer-function $G(s)$ is small in the frequency range of interest, the transfer function from the actuator input to the actual force output then becomes

$$\frac{u}{v} = -ms\left[1 + \frac{ms^2 + k}{Ks[1 + ms^2G(s)]}\right]^{-1} = -\frac{ms}{Ts + 1} \tag{12}$$

where $T = m/K$ ($1/T$ is the actuator high-pass break frequency).

The actuator to be used for the COFS-I has a high-pass break frequency of about 1 Hz.[1] This frequency must be distinguished from the 110-Hz actuator bandwidth given in Ref. 1. The low-frequency characteristics given by Eq. (12) are more important than the 110-Hz bandwidth because of the frequency range of the primary bending modes of interest in the control design. The first bending mode of 0.18 Hz is within the high-pass break frequency and the second bending mode of 1.98 Hz is near the break frequency. Special care should be taken about the high-pass filtering characteristics of the proof-mass actuator dynamics for the COFS-I flight experiment.

In Ref. 16 a second-order high-pass filter characteristic is reported for the microprocessor-controlled proof-mass actuator. The experimental frequency response data in Ref. 16 also shows an additional oscillatory actuator mode between 0.1 and 1 Hz. Such additional dynamics of the actuator, if not included in the controller design, may lead to control instabilities even in the colocated control experiment. Experimental frequency response data of the actuator and a detailed model including the actuator stroke and force limit should be used for the detailed control design of the COFS-I. In this paper, a first-order high-pass filter model given by Eq. (12) is assumed for the preliminary control design.

Microprocessor Computational Delay Effect

The microprocessor sampling rate of 150 Hz (6.6-ms sampling period) for the COFS-I is relatively fast compared to the sampling rates of the current flight computers (40–100 ms). However, the time-delay effect is discussed here for the COFS-I, since an accurate modeling of the control-loop time delay becomes especially critical when a phase stabilization, as opposed to a gain stabilization, is used for flexible-mode stabilization.

For the s-domain control synthesis[7–9] the pure time delay and the sample/ZOH (zero-order-hold) delay can be approximated as

$$e^{-Ts} = \frac{T^2s^2/8 - Ts/2 + 1}{T^2s^2/8 + Ts/2 + 1} \qquad \text{(pure time delay)} \quad (13)$$

$$\frac{1 - e^{-Ts}}{Ts} = \frac{1}{T^2s^2/12 + Ts/2 + 1} \qquad \text{(sample/ZOH delay)} \quad (14)$$

For a relatively fast sampling rate, the sample/ZOH delay can be approximated as $T/2$-s pure delay. The phase lag at frequency ω (rad/s) due to pure time delay T (s) is simply given by

$$\text{phase-lag angle (deg)} = 57.3T\omega \qquad (15)$$

For example, the phase-lag angles due to an effective delay of 10 ms at the first (1.14 rad/s), second (12.3 rad/s), third (38.6 rad/s), and fourth (79.8 rad/s) modes are 0.65, 7.04, 21.9, and 45.7 deg, respectively. The effects of the 10 ms delay on the first and second modes can clearly be ignored. Since the third and fourth modes are difficult to observe and control, the delay effects on these high-frequency modes can also be ignored. However, it will be useful to have on-orbit experiments with significant computational delay (> 50 ms) in order to investigate the effects of time delay on the closed-loop stability.

A Generalized Structural Filtering Concept

A control synthesis for flexible structures must consider the parameter uncertainties, the unmodeled dynamics, the actuator/sensor dynamics, and the control-loop time delay. The classical concepts of gain/phase stabilization are very useful for designing a robust compensator and for evaluating robustness to the model uncertainties. A nonminimum-phase filter designed using the generalized structural filtering concept is proposed for the COFS-I flight experiment. This new structural filtering concept for flexible-mode stabilization[7] is primarily based on the classical gain/phase stabilization concepts that are briefly discussed as follows:

1) A gain-stabilized mode is one that is closed-loop stable for the selected loop gain and assumed passive damping ratio, but can become unstable if the gain is raised or the damping ratio is reduced. Hence, it has finite-gain margin but is closed-loop stable regardless of the phase uncertainty.

2) A phase-stabilized mode is one which, for an arbitrarily small passive damping ratio, is closed-loop stable. It has a finite-phase margin.

Two approaches to stabilize the flexible modes are possible from the classical control viewpoint. The first of these is a gain stabilization approach in which notch filtering is used. The gain stabilization only provides the necessary attenuation of the flexible modes to be suppressed in the control loop. It does not increase the closed-loop damping ratio; although it is closed-loop stable regardless of the phase uncertainty, the gain stabilization can become very sensitive to frequency variations. A practical example of notch filtering for flexible-mode stabilization is the scan platform controller design for the Galileo spacecraft.[10] A double-notch filter is employed to suppress the unstably interacting flexible mode in the scan platform loop with a noncolocated actuator and sensor pair.

The second approach to flexible-mode stabilization is phase stabilization. The phase stabilization, as opposed to the gain stabilization, provides the proper phasing to increase the closed-loop damping of the flexible modes. The amount of active damping depends upon the type of phase stabilization. If a significant gain attenuation is accompanied with phase stabilization, the closed-loop damping ratio will not be increased much. Roll-off filtering often results in such phase stabilization with insignificant active damping.

In certain cases, a phase stabilization is more desirable as its stability does not depend upon the passive damping ratio, a parameter whose value is rarely known with any precision. However, the phase stabilization can become sensitive to the phase uncertainty and the parameter variations. A practical case of employing a complex phase-lead filter (that is often misleadingly called a notch filter) to provide the necessary phase lead to the flexible mode is the scan platform control of the OSO-8 spacecraft using a noncolocated actuator and sensor pair.[11]

In general, the classical gain/phase stabilization concepts are very useful for designing a robust compensator. The classical structural filtering concepts described above are now significantly enhanced by the new concept of generalized structural filtering, especially with nonminimum-phase zero.[17] A generalized second-order filter with arbitrary complex poles and zeros can be simply represented as

$$\frac{s^2/\omega_z^2 + 2\zeta_z s/\omega_z + 1}{s^2/\omega_p^2 + 2\zeta_p s/\omega_p + 1} \qquad (16)$$

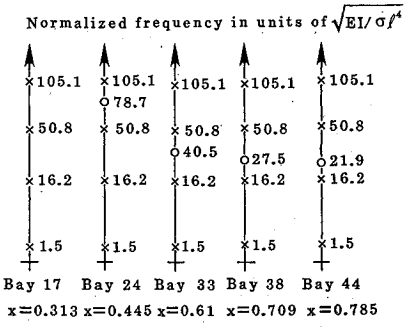

Fig. 4 Poles and zeros of transfer functions from the tip actuator to the beam deflection at various sensor locations.

By different choices of the coefficients several well-known frequency shaping filters can be obtained. For $\omega_z = \omega_p$ and $\zeta_z = 0$ we have a notch filter for gain stabilization. The notch sharpness depends on the damping ratio of the notch pole (usually $\zeta_p = 0.5$–1.0). Great care must be excercised in selecting the parameters of the notch filter because of its phase lag at low frequency and its sensitivity to frequency uncertainty. For $\omega_p > \omega_z$ (and usually $\zeta_p = \zeta_z$), we have a complex phase-lead filter for phase stabilization. The amount of phase lead depends primarily on the ω_p/ω_z ratio, but the ratio should not be too high because of the gain increase at higher frequencies. Without the filter zeros we have a simple roll-off filter.

Those filters discussed above are minimum phase i.e., the filter poles and zeros are on the left-half s-plane. However, a variety of nonminimum-phase filters ($\zeta_z < 0$) developed by Wie and Byun[7] have very interesting gain/phase characteristics that are useful for flexible-mode stabilization. Because of such generalized structural filtering concept, the classical direct-frequency-shaping technique based on the gain/phase stabilization concepts is now significantly enhanced. A practical procedure for synthesizing a robust compensator using nonminimum-phase filters can be found in Ref. 7. The nonminimum-phase filtering, as oppossed to the minimum-phase filtering, provides the proper phasing to increase the closed-loop damping ratio of the flexible modes while maintaining a good robustness property to the model uncertainty. The use of such nonminimum-phase filters for the second-mode stabilization of the COFS-I using a noncolocated actuator and sensor pair is proposed for the COFS-I flight experiment.

Next, the colocated control synthesis followed by noncolocated control synthesis of the COFS-I is discussed.

Control Using the Tip-Mounted Actuator/Sensor

A simplified control-loop block diagram is shown in Fig. 5; effective control-loop delay of 10 ms from microprocessor implementation is assumed. A first-order high-pass filter model of the proof-mass actuator given by Eq. (12) is also assumed. An eighth-order transfer-function model with a 0.002 modal damping ratio and with a $\pm 25\%$ pole-zero uncertainty is considered as a preliminary control-design model, while the rate gyro and accelerometer are assumed as ideal sensors. Control using the tip-mounted actuator and accelerometer pair is considered here; the rate-gyro loop that controls the tip slope can also be analyzed similarly as the accelerometer loop. Feedback of the translational and/or rotational velocity with proportional-and-integral (PI) compensation is a basic scheme to actively control the flexible modes using the colocated actuator and sensor. The PI control is needed to effectively compensate the high-pass filtering characteristics of the proof-mass actuator. The PI compensator zero can be chosen near the actuator pole at $s = -6.28$ (the actuator high-pass break frequency). A mismatching of the actuator pole by the PI compensation will not be significant.

Figure 6 shows a normalized impulse response of the colocated control. A low gain is selected since the primary actuator has been sized to provide a maximum damping ratio of 5% for the first bending mode.[1] From Fig. 6 we notice the dominance of the first mode. The open-loop Bode magnitude plot for this low-gain case is shown in Fig. 7, which also illustrates the dominance of the first bending mode. Figure 8 shows the locus of closed-loop poles vs overall loop gain. Since the third and fourth modes are difficult to be affected by the active control, they are not shown in the root-locus plot. In other words, the third and higher modes are gain-stabilized and they may be completely ignored for the active control design.

Figure 9 shows an impulse response of the same controller with an increased loop gain. It is evident that rapid transient control was achieved. The first mode has a 53% active damping ratio and all the higher modes are stable. Such rapid transient control may not be possible because of the actuator saturation.[1] It is, however, assumed here that either the actual structural deflection is within the actuator stroke limit or that a new improved actuator is available for high-gain control-law testing.

Control Using the Noncolocated Actuator/Sensor

Noncolocated actuator/sensor control ("noncolocated control" for short), in general, is not as simple as colocated con-

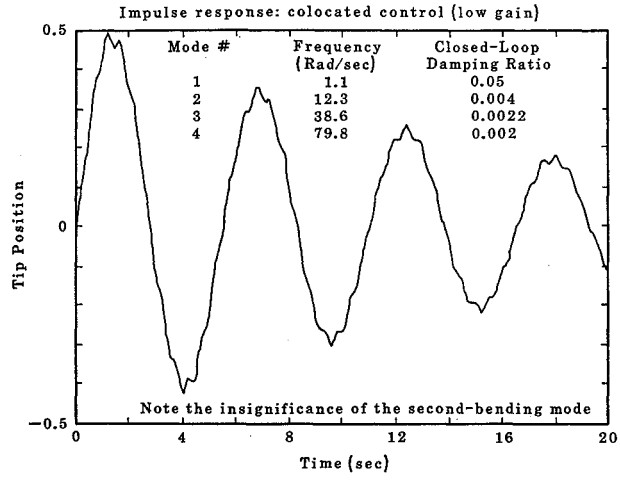

Fig. 6 An impulse response of the colocated control (low gain).

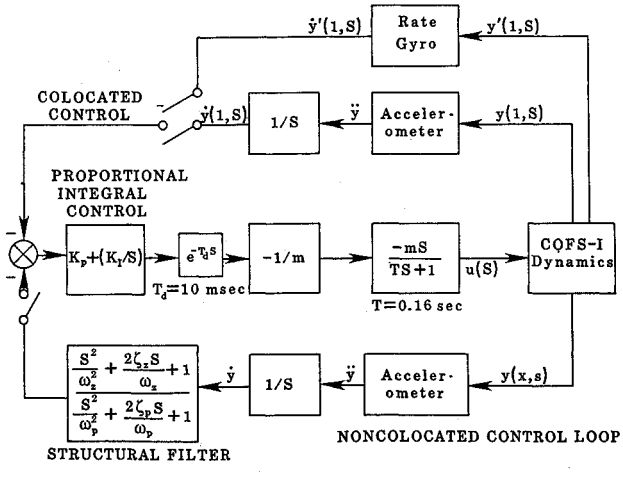

Fig. 5 A simplified control-loop block diagram.

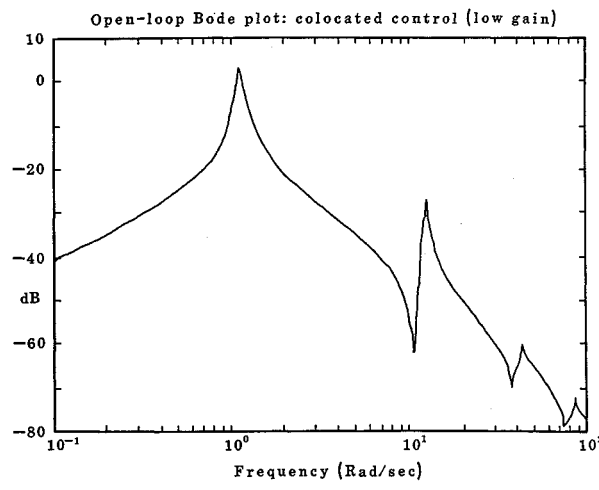

Fig. 7 Open-loop Bode plot of the colocated control (low gain).

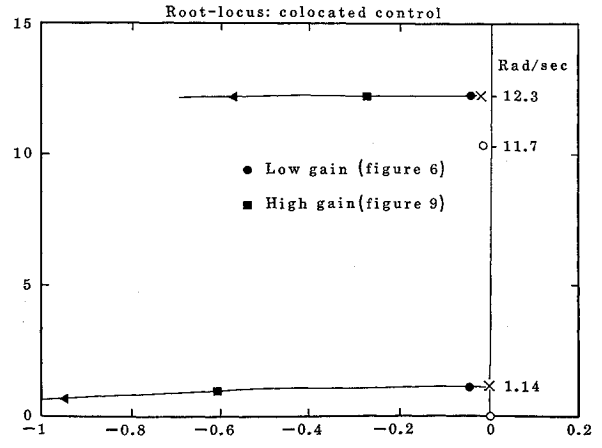

Fig. 8 Root-locus vs overall loop gain (colocated case).

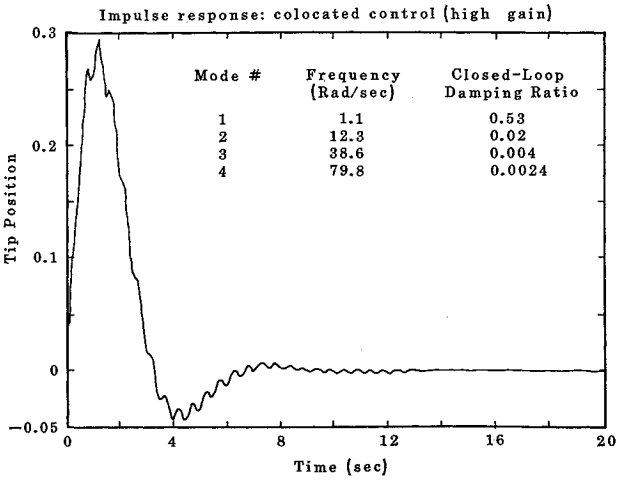

Fig. 9 An impulse response of the colocated control (high gain).

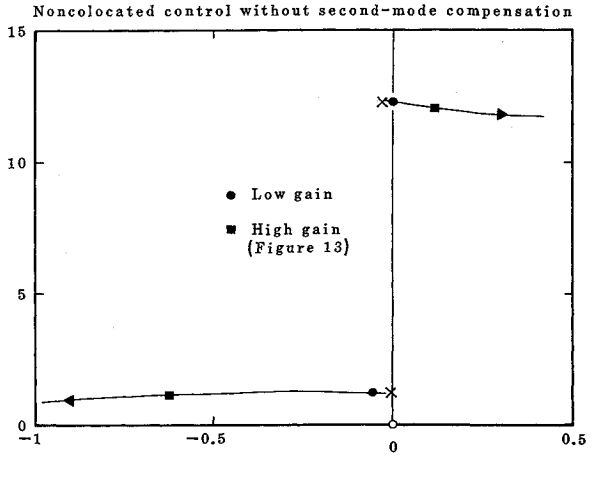

Fig. 10 Root-locus vs overall loop gain (nonlocated control).

trol, because of the unstable interactions between modes. Practical examples of noncolocated control are the scan platform control of the Galileo[10] and OSO-8[11] spacecraft, where the actuator and sensor are not colocated because of some physical constraints. For these flexible spacecraft the classical notch and phase lead/lag filtering techniques were used.

Application of the standard linear-quadratic-gaussian (LQG) technique to this kind of problem often results in a feedback compensator that is of high order and sensitive to

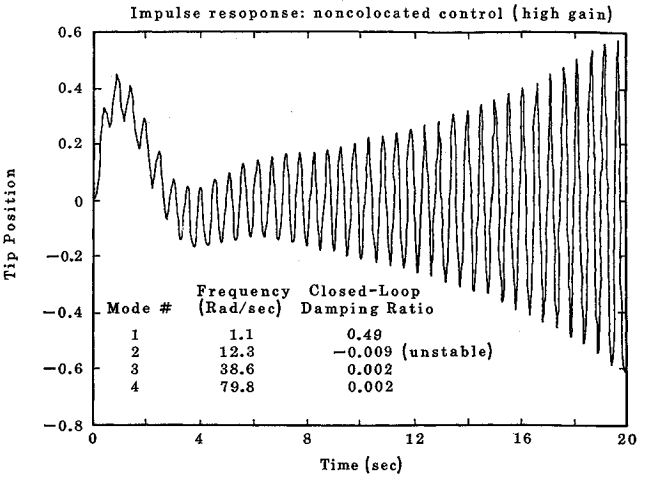

Fig. 11 An impulse response of the noncolocated control without second-mode compensation.

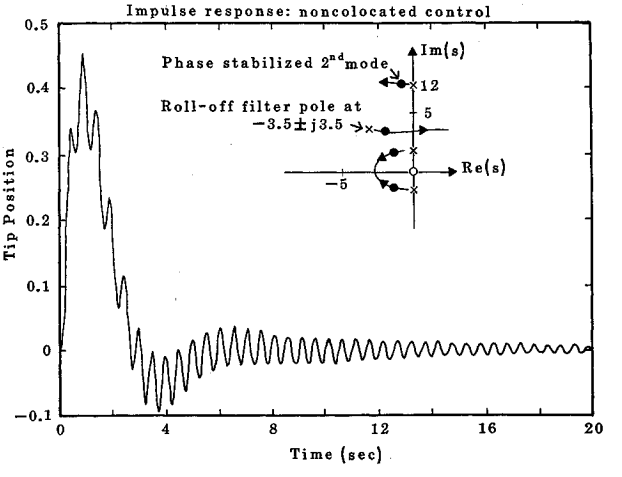

Fig. 12 Noncolocated control with roll-off filtering.

model uncertainty.[17,18] Many ways of improving the robustness of the LQG design have been proposed and applied to the noncolocated control problem (e.g., see Ref. 19). The contribution of this paper is to apply the generalized structural filtering concept[7] to the noncolocated problem of the COFS-I and to demonstrate the simplicity and practicality of the classical control approach.

A noncolocated control experiment, by controlling the beam structure using the tip-mounted actuator and the noncolocated sensor (accelerometer) at bay 33, is proposed for the COFS-I flight experiment. The primary objective of the proposed experiment is to flight-test various structural filters (e.g., notch, phase lead/lag, nonminimum-phase filters, etc.), and to identify the most robust filtering technique to be used for the active vibration control of future large space structures. In particular, this noncolocated control experiment as opposed to the colocated control experiment will generate an important technology data base that will provide the control designer with options and approaches to practical implementation of active vibration control systems.

Assuming an ideal integration of the accelerometer output, preliminary control analysis and design can be performed for the noncolocated control of the COFS-I. Velocity feedback with the PI compensation results in a decreased closed-loop damping ratio for the second mode as shown in Fig. 10. The loop gain is selected to provide a 5% damping ratio to the first mode because of the actuator limitation. With such low gain, the second mode is gain stabilized, as can be seen from the

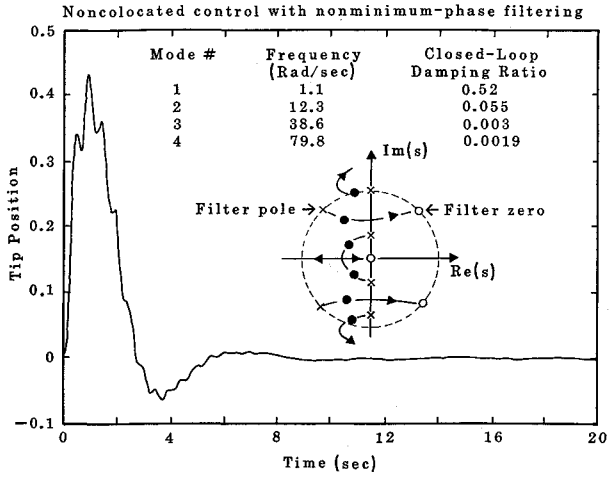

Fig. 13 Noncolocated control with nonminimum-phase filtering.

figure. For a high loop gain, the second mode becomes unstable, while the first mode has a 49% active damping ratio as can be seen in Fig. 11. Because of actuator limitation and nonlinearity, such instability may not be experienced.

Assuming either that an improved actuator is available or that the actual structural vibration level is within the actuator stroke limit, two different structural filters for the second-mode stabilization have been studied. Figure 12 shows the root locus and an impulse response of the noncolocated control case with simple roll-off filtering. The second mode is phase-stabilized, but it has a small active damping ratio due to the gain attenuation by the roll-off filter. Figure 13 shows the root locus and transient response for the noncolocated control with nonminimum-phase filtering of the second bending mode; not much second-mode "ringing" can be observed. The non-minimum-phase filter provides the proper phasing (approximately 180-deg lag) of the second mode signals at 12 rad/s to increase the closed-loop damping ratio, while maintaining good performance and robustness to parameter variations. The closed-loop system has a 12 dB gain margin and is stable to the $\pm 25\%$ frequency uncertainty; both the first and the second modes have more than 50-deg phase margins.

Comparing Fig. 9 (colocated control) and Fig. 13 (noncolocated control with nonminimum-phase filtering), it is concluded that we can achieve the same performance as the colocated control, even when the actuator and sensor cannot be colocated because of some physical constraints.

Conclusions

Preliminary results of pole-zero modeling and active vibration control synthesis for the COFS-I are presented. This paper has demonstrated the simplicity and practicality of a classical transfer-function approach enhanced by the nonminimum-phase filtering concept. This paper has shown that the COFS-I can be an excellent generic testbed for validating the proposed active vibration control scheme for the case when the actuator and sensor cannot be colocated due to some physical constraints. It is hoped that the preliminary results obtained using the analytical pole-zero model of the COFS-I truss structure will contribute to advancing the structural modeling and control technologies through actual flight experiments.

References

[1]*Control of Flexible Structures (COFS) Technology Program*, NASA Langley Research Center, Hampton, VA, Feb. 1986.

[2]Wie, B., "On the Modeling and Control of Flexible Space Structures, SUDDAR 525," Ph.D. Dissertation, Dept. of Aeronautics and Astronautics, Stanford Univ., Stanford, CA, June 1981.

[3]Wie, B. and Bryson, A. E., Jr., "Modeling and Control of Flexible Space Structures," *Proceedings of the 3rd VPI & SU/AIAA Symposium on the Dynamics and Control of Large Flexible Spacecraft*, Blacksburg, VA, June 1981, pp. 153–174.

[4]Breakwell, J. A., "Optimal Control of Distributed Systems," *Journal of the Astronautical Sciences*, Vol. 29, No. 4, Oct.–Dec. 1981, pp. 343–372.

[5]Skaar, S. B., "Closed Form Optimal Control Solutions for Continuous Linear Elastic Systems," *Journal of the Astronautical Sciences*, Vol. 32, No. 4, Oct.–Dec. 1984.

[6]Wie, B. and Bryson, A. E., Jr., "Pole-Zero Modeling of Flexible Space Structures," 1987 American Control Conf., June 1987; *Journal of Guidance, Control, and Dynamics* (to be published).

[7]Wie, B. and Byun, K., "A New Concept of Generalized Structural Filtering for Active Vibration Control Synthesis," *Proceedings of the AIAA Guidance, Navigation, and Control Conference*, AIAA, New York, Aug. 1987; also, *Journal of Guidance, Control, and Dynamics* (to be published).

[8]Wie, B. and Plescia, C. T., "Attitude Stabilization of a Flexible Spacecraft During Stationkeeping Maneuvers," *Journal of Guidance, Control, and Dynamics*, Vol. 7, July–Aug. 1984, pp. 430–436.

[9]Wie, B., Lehner, J. A., and Plescia, C. T., "Roll/Yaw Control of a Flexible Spacecraft Using Skewed Bias Momentum Wheels," *Journal of Guidance, Control, and Dynamics*, Vol. 8, July–Aug. 1985, pp. 447–453.

[10]Chodas, J. L. and Man, G. K., "Design of the Galileo Scan Platform Control," *Journal of Guidance, Control, and Dynamics*, Vol. 7, July–Aug. 1984, p. 422.

[11]Yocum, J. F. and Slafer, L. I., "Control System Design in the Presence of Severe Structural Dynamics Interactions," *Journal of Guidance and Control*, Vol. 1, March–April 1978, pp. 109–116.

[12]Wie, B. and Bryson, A. E. Jr., "On Multivariable Control Robustness Examples: A Classical Approach," *Journal of Guidance, Control, and Dynamics*, Vol. 10, Jan.–Feb. 1987, pp. 118–120.

[13]Mitchell, J. R. and Lucas, J. C., "1-CAT: A MIMO Design Methodology," NASA CP-2467, 1986, pp. 293–333.

[14]"ACOSS Twelve (Active Control of Space Structures)," Final Technical Report, Lockheed Missiles & Space Co., Feb. 1984, RADC-TR-84-28.

[15]"ACOSS Five (Active Control of Space Structures) Phase 1A," Final Technical Report, Lockheed Missiles & Space Co., March 1982 RADC-TR-82-21.

[16]Zimmerman, D. C., Horner, G. C., and Inman, D. J., "Microprocessor Controlled Force Actuator," *Proceedings of AIAA/ASME/ASCE/AHS 27th Structures, Structural Dynamics, and Materials Conference*, New York, 1986.

[17]Cannon, R. H. and Rosenthal, D. E., "Experiments in Control of Flexible Structures with Noncolocated Sensors and Actuators," *Journal of Guidance, Control, and Dynamics*, Vol. 7, Sept-Oct. 1984, p. 546.

[18]Bryson, A. E. Jr., "Some Connections between Classical and Modern Control Concepts," *ASME Journal of Dynamic Systems, Measurements, and Control*, June 1979, pp. 91–98.

[19]Bryson, A. E. Jr., Hermilin, S., and Sun, J. L. C., "LQG Controller Design for Robustness," American Control Conference, Seattle, WA, June 1986.